

~~UNCLASSIFIED~~

SECURITY CLASSIFICATION OF THIS PAGE (When Data Entered)

ARO 16513.6-PH

REPORT DOCUMENTATION PAGE		READ INSTRUCTIONS BEFORE COMPLETING FORM
1. REPORT NUMBER	2. GOVT ACCESSION NO.	3. RECIPIENT'S CATALOG NUMBER
		A125940
4. TITLE (and Subtitle) Search for Far Infrared Radiation From Optically Pumped Defect Modes		5. TYPE OF REPORT & PERIOD COVERED Final Technical Report Sept. 3/79 - Dec. 31/82
7. AUTHOR(s) A.J. Sievers		6. PERFORMING ORG. REPORT NUMBER DAAG-29-79-C-0170
9. PERFORMING ORGANIZATION NAME AND ADDRESS Laboratory of Atomic and Solid State Physics Cornell University Ithaca, NY 14853		10. PROGRAM ELEMENT, PROJECT, TASK AREA & WORK UNIT NUMBERS
CONTROLLING OFFICE NAME AND ADDRESS U. S. Army Research Office Post Office Box 12211 Research Triangle Park, NC 27709		12. REPORT DATE
MONITORING AGENCY NAME & ADDRESS (if different from Controlling Office)		13. NUMBER OF PAGES
		15. SECURITY CLASS. (of this report) Unclassified
		15a. DECLASSIFICATION/DOWNGRADING SCHEDULE
DISTRIBUTION STATEMENT (of this Report)  Approved for public release; distribution unlimited.		
DISTRIBUTION STATEMENT (of the abstract entered in Block 20, if different from Report)  NA		
16. SUPPLEMENTARY NOTES The view, opinions, and/or findings contained in this report are those of the author(s) and should not be construed as an official Department of the Army position, policy, or decision, unless so designated by other documentation.		
18. KEY WORDS (Continue on reverse side if necessary and identify by block number) IR Optical Pumping, vibrational relaxation dynamics, matrix isolated molecules, incoherent laser saturation, hole burning spectroscopy, anharmonic decay, ground state optical pumping, and persistent spectral holes.		
19. ABSTRACT (Continue on reverse side if necessary and identify by block number) The vibrational relaxation dynamics of a spherical top molecule embedded in alkali halide crystals have been investigated under conditions of non-equilibrium IR laser excitation. Incoherent laser saturation and high resolution hole burning spectroscopy have been used to measure the anharmonic decay of the excited vibrational state. In addition persistent IR spectral holes (with lifetimes greater than 10 minutes at 1.4°K) have been observed, indicating for the first time the presence of ground state optical pumping processes for a high		

DTIC FILE COPY

DD FORM 1 JAN 73 1473

EDITION OF 1 NOV 65 IS OBSOLETE

UNCLASSIFIED

13 08 21

15

SECURITY CLASSIFICATION OF THIS PAGE (When Data Entered)

symmetry impurity in a cubic lattice. Our discoveries of long-lived vibrational modes in alkali halide crystals points to a new avenue of research on the physics of solids and also supports the premise that IR optical pumping can occur in the vibrational mode spectrum of a solid.

Search for Far Infrared Radiation  
From Optically Pumped Defect Modes

Final Technical Report

A.J. Sievers

February 9, 1983

U.S. Army Research Office

Grant No. DAAG-29-79-C-0170

Laboratory of Atomic and Solid State Physics

Cornell University  
Ithaca, New York 14853

Approved for Public Release

Distribution Unlimited

Approved for Public Release

Accession For			
NTIS GRAM	<input checked="" type="checkbox"/>		
DTIC TAB	<input type="checkbox"/>		
Unpublished	<input type="checkbox"/>		
Justification			
By			
Distribution			
Approved for Public Release			
Dist	<input type="checkbox"/>	<input type="checkbox"/>	<input type="checkbox"/>
A		<input type="checkbox"/>	<input type="checkbox"/>

## TABLE OF CONTENTS

I.	PROJECT SUMMARY . . . . .	2
II.	PROGRESS REPORT . . . . .	4
	A. Introduction . . . . .	4
	B. Vibrational Relaxation Dynamics of CO <sub>2</sub> Laser Excited ReO <sub>4</sub> <sup>-</sup> Ions in Alkali Halide Lattices . . . . .	10
	1. Medium and high resolution spectroscopy. . . . .	10
	2. Coincidences with CO <sub>2</sub> laser lines. . . . .	12
	3. Incoherent saturation. . . . .	14
	4. IR hole burning. . . . .	19
	5. The persistent hole. . . . .	23
	C. Paraelectric Centers in Li Doped Alkali Halide Crystals. .	29
	D. CO <sub>2</sub> Laser Saturation of Local Modes in CaF <sub>2</sub> :H <sup>-</sup> :Er <sup>3+</sup> . . . .	33
	E. ARO Sponsored Publications . . . . .	39
	F. Participating Scientific Personnel . . . . .	42
	G. References . . . . .	43

## I. PROJECT SUMMARY

During the past three years one of our principle efforts has been to unravel the details of the vibrational relaxation dynamics of a spherical top molecule embedded in a crystalline lattice. The techniques of incoherent laser saturation and infrared hole-burning spectroscopy were used to discover the microscopic mechanisms responsible for the decay of the excited vibrational state. The results of these investigations show that at low temperature the decay channel consists of multistep emission of other internal modes, localized phonon modes and band phonons. The intrinsic symmetry and simplicity of this hole burning system has enabled us to determine many aspects of anharmonic decay processes and to predict that other modes in solids may have vibrational Q's as large as  $10^{12}$ .

In the course of these hole burning experiments, an unusual new effect was observed: the burning of persistent holes in a vibrational mode at extremely low powers. These long-lived holes have dark lifetimes of 10 minutes or longer, and indicate that the vibrational ground state may possess two or more distinct configurations. Ground state optical pumping seems to occur via a photon induced reorientation process, which explains the burning of these holes at laser intensities many orders of magnitude below the usual excited state saturation intensity.

These persistent hole measurements complement the earlier studies on electronic transitions in organic glasses and alkali halides. We conclude that the burning of such holes at low laser intensity is a general solid state phenomenon which can occur whenever the complete ground state of the system to be excited has configurational degeneracy. An analogy may exist between the IR vibrational mode hole burning and the aggregate color

center hole burning in the optical region which has been suggested as a new method for high density optical storage.

Our discoveries of long-lived excited states and configurationally degenerate ground states of vibrational modes are particularly important steps in the study of vibrational energy transfer in solids. It is now clear that the ultrahigh resolution laser techniques which have provided so much information about electronic states have an analogue for the study of anharmonic interactions in almost any lattice-defect combination.

One of the technological spin offs from our study of the nonlinear properties of isolated spherical top molecules in solids is the discovery that the longitudinal optic mode of a thin film of KReO<sub>4</sub> can be saturated at room temperature. This arrangement may have applications as a saturable mirror or as 90° switch.

In addition to the IR laser work described above considerable effort has gone into making near mm spectroscopic measurements on a variety of solids at low temperatures. Particularly significant are the studies on paraelectric centers in doped alkali halides and the crystalline field levels in rare earth doped alkaline earth fluorides. From these measurements we have isolated three different kinds of local vibration-defect interactions which have a near mm wave electric dipole moment and deserve further study. They are vibrational-tunneling, vibrational-rotational and vibrational-crystal field.

During the past three years twenty-eight publications and two theses have resulted from this program.

## II. PROGRESS REPORT

### A. Introduction

The discovery that a tetrahedral molecule,  $\text{ReO}_4^-$ , could be doped into alkali halide crystals and also that at room temperature the molecule could be driven far from equilibrium by a resonant  $\text{CO}_2$  laser field<sup>1-3</sup> has made possible a number of new experiments on the nonequilibrium dynamics of defects in solids. Our main thrust during the past three years has been to learn how the  $\text{CO}_2$  energy given to the molecule is transferred to the lattice at low temperatures.

Knowledge of the relaxation mechanisms for  $\text{ReO}_4^-$  molecules in alkali halides is important for the following reasons. First, the relaxation dynamics of molecules in solids are expected to differ greatly from those for molecules in the gaseous state. Isolation in a solid matrix may hinder or quench the usual rotational degrees of freedom and allow bare vibrational modes to be studied without coupling to rotation. Further, inhomogeneous broadening in solids is produced by static strains rather than by dynamic Doppler broadening. Moreover, the properties of isolated molecules are easily studied in solid solutions, without the necessity of using extremely low pressures to reduce molecular collisions. The presence of a new bath of excitations, phonons, generates new interactions and processes. All of this means that the study of vibrational relaxation phenomena for molecules in solids can lead to the discovery of novel physical mechanisms.

Secondly,  $\text{ReO}_4^-$  molecules in alkali halides are representative of a class of systems with important practical applications: solid state saturable absorbers. Such systems can be used for laser mode-locking,<sup>2</sup>

pulse shaping,<sup>4</sup> and four-wave mixing,<sup>3</sup> for example. The study of  $\text{ReO}_4^-$  in solids may lead to new nonlinear applications for these materials.

Lastly, knowledge of the relaxation dynamics of this spherical top molecule provides an important foundation for future studies of symmetric top molecules. Because the latter systems possess a permanent dipole moment, they may provide new sources for tuneable far infrared radiation. The vibrational decay and dephasing mechanisms for symmetric top molecules in ionic crystals may be similar to those for  $\text{ReO}_4^-$  ions in alkali halides.

During the past three years our efforts have focused on unraveling the details of the vibrational relaxation dynamics of the  $\text{ReO}_4^-$  alkali halide system at liquid helium temperatures. The techniques of incoherent laser saturation and infrared hole-burning spectroscopy have been utilized here to discover the microscopic mechanisms responsible for the lifetime ( $T_1$ ) and homogeneous dephasing ( $T_2$ ) processes for the  $v_3$  mode. The results of these investigations show that below 10 K, the decay channel consists of a complex, multistep emission of other internal modes, localized phonon modes, and band phonons. Above 10 K, the dephasing time  $T_2$  is controlled by acoustic phonon scattering, while below 10 K,  $T_2$  is lifetime limited.

In the course of these experiments, an unusual new effect was observed: the burning of persistent holes in the  $v_3$  mode absorption at extremely low powers. These long-lived holes have dark lifetimes of 10 minutes or longer, and indicate that the vibrational ground state may possess two or more distinct levels corresponding to different orientations of the molecule. Ground state optical pumping seems to occur via a photon-

induced reorientation process, which explains the burning of these holes at intensities many orders of magnitude below the usual saturation intensity. Figure 1 schematically indicates the range of intensities involved.  $KCl:ReO_4^-$  saturates according to a homogeneous model with characteristic intensity of  $1 \text{ MW/cm}^2$  at room temperature. By contrast,  $RbI$  saturates inhomogeneously with a saturation parameter of roughly  $1 \text{ W/cm}^2$  at  $1.4 \text{ K}$ . The long-lived hole generated by ground state optical pumping can be observed at any intensity below roughly  $10 \text{ mW/cm}^2$ , with a growth rate determined by photon flux. The  $ReO_4^-$  - alkali halide system clearly possesses a rich variety of phenomena spanning nearly 15 orders of magnitude of intensity.

Figure 2 illustrates the types of experiments which were required to identify the physical processes. In the next section we shall first describe the high resolution measurements then consider the important problem of producing useable coincidences with  $CO_2$  laser lines. These coincident systems form the foundation upon which all the other experiments have been based. Next measurements of the saturation parameter for all hosts will be presented from which values for the product of the two level system relaxation times  $T_1$  and  $T_2$  are derived. These measurements will allow the determination of the exact decay channel for the  $v_3$  vibrational mode. Finally the various hole burning experiments will be described. We conclude this section with a brief description of saturation measurements on  $KReO_4$  thin films evaporated onto dielectric windows.

In addition to the  $10 \mu$  wavelength work described above considerable effort has gone into making near mm wave spectroscopic measurements on a variety of solids at low temperatures. Studies have been

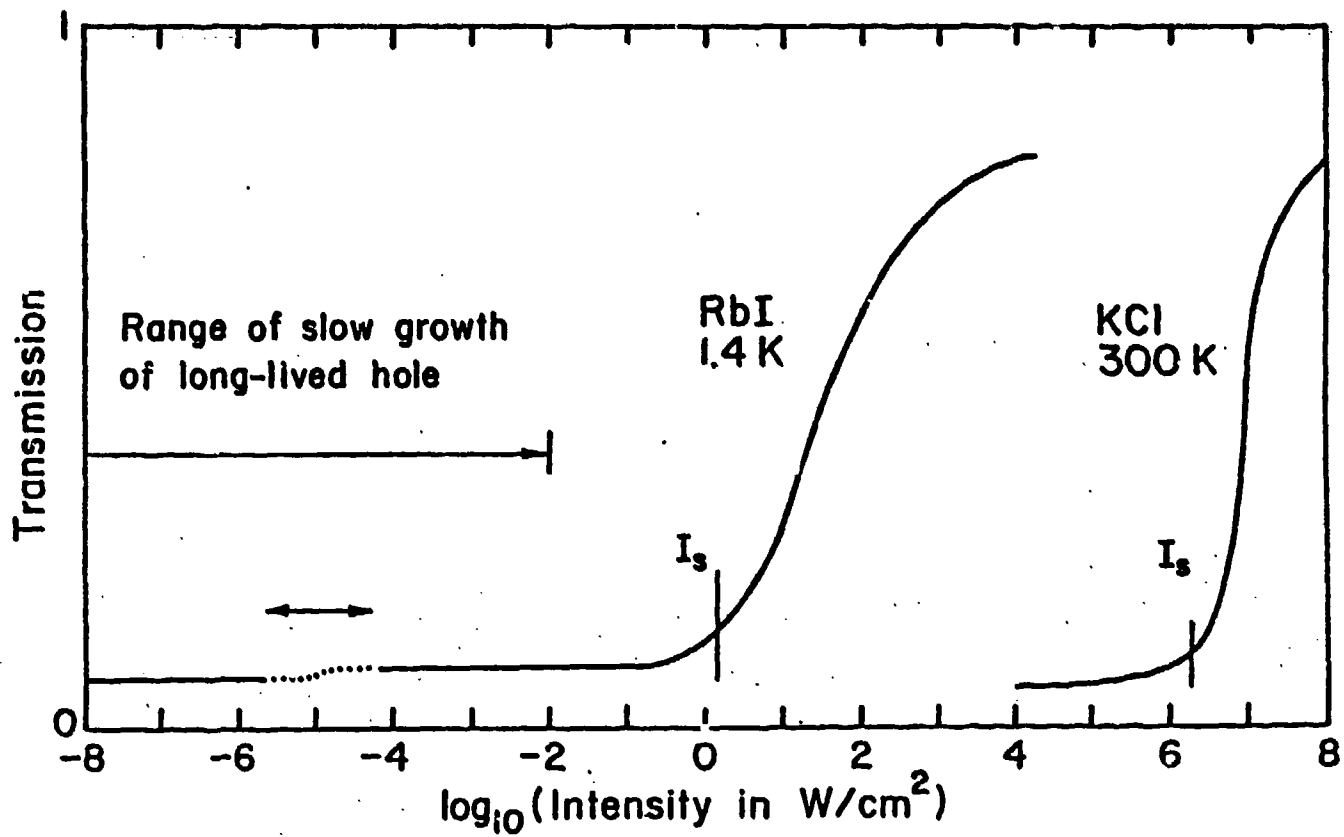


Figure 1. Illustration of the wide range of intensities involved in studying the nonlinear properties of vibrational modes in solids. long-lived hole growth and erasing effects are observed at power levels below  $\sim 10 \text{ mW/cm}^2$ . RbI at 1.4 K saturates inhomogeneously with  $I_s \sim 1 \text{ W/cm}^2$ . KCl at 300 K saturates with  $I_s \sim 1 \text{ MW/cm}^2$ . The dotted lines indicate that long-lived hole growth can be easily observed at virtually any intensity less than  $10^{-2} \text{ W/cm}^2$ .

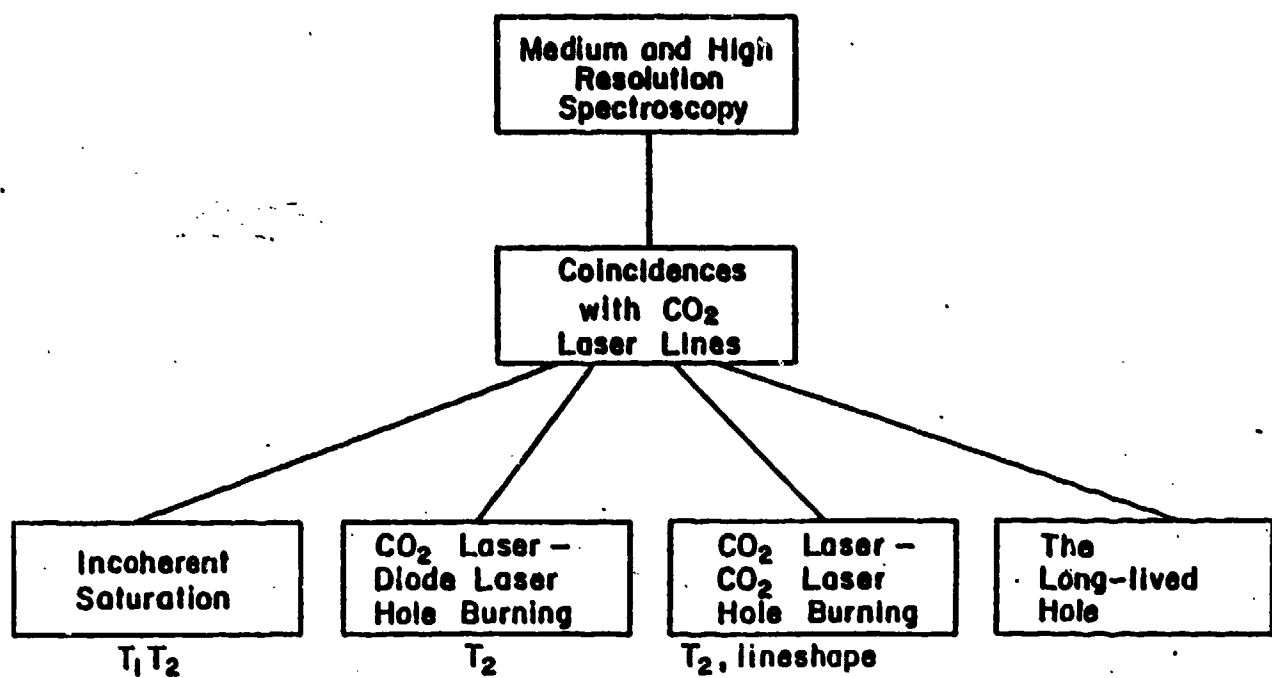


Figure 2. Summary of IR Experiments Required to identify vibrational relaxation dynamics of  $\text{ReO}_4^-$  in alkali halides.

made on ultrafine metallic particles, fluctuating valence metals and alloys, shallow electronic traps in doped germanium, paraelectric centers in doped alkali halide crystals and crystalline field levels in rare earth doped alkaline earth fluorides. These latter two systems are of particular interest because they not only possess energy states in the near mm wave region but also additional energy levels at CO<sub>2</sub> laser frequencies so we shall describe these studies in some detail.

A complete description of these various efforts can be found in the publications listed at the end of this chapter. Two Ph.D. theses were completed during this three year period.<sup>5,6</sup>

## B. Vibrational Relaxation Dynamics of CO<sub>2</sub> Laser Excited ReO<sub>4</sub><sup>-</sup> in Alkali Halide Lattices

### 1. Medium and high resolution spectroscopy

A variety of medium resolution ( $0.5 \text{ cm}^{-1}$ ) and high resolution ( $3 \times 10^{-4} \text{ cm}^{-1}$ ) spectroscopic studies of the  $\nu_3$  mode of ReO<sub>4</sub><sup>-</sup> molecules in alkali halides have been made at low temperatures. Low power transmission spectra such as these provide important background information regarding lineshapes and line splittings; information which is crucial to the interpretation of the high power saturation and hole burning experiments to be described later. Furthermore, temperature dependent linewidth measurements of the KI:ReO<sub>4</sub><sup>-</sup> absorption provide precise information about the dominant dephasing ( $T_2$ ) mechanism for these systems.

The low temperature measurements at medium resolution showed that the ReO<sub>4</sub><sup>-</sup>  $\nu_3$  absorption line in all pure hosts is a sharp, isotope-split doublet with an instrumental resolution limited width.

The loan from G.M. of a Pb<sub>1-x</sub>Sn<sub>x</sub>Te semiconductor diode laser, with a resolution on the order of 10 MHz, provides the high resolution data.<sup>7</sup> Figure 3 shows the absorption spectrum at 2.06°K of an unannealed sample of KI + 0.001% KReO<sub>4</sub>. This spectrum is for the <sup>187</sup>Re isotope. Each component of the triplet has a width of approximately  $0.02 \text{ cm}^{-1}$ . Upon annealing at 600°C for 2 hours, the triplet structure disappears, leaving a single very narrow line of  $0.016 \text{ cm}^{-1}$  width. The line shape is gaussian at this temperature indicating that the absorption is inhomogeneously broadened. These results demonstrate that at low temperatures the  $\nu_3$  mode of <sup>187</sup>ReO<sub>4</sub><sup>-</sup> in pure KI misses coincidence with the P(42) CO<sub>2</sub> laser line by approximately  $0.22 \text{ cm}^{-1}$ . The reason for the appearance of the triplet

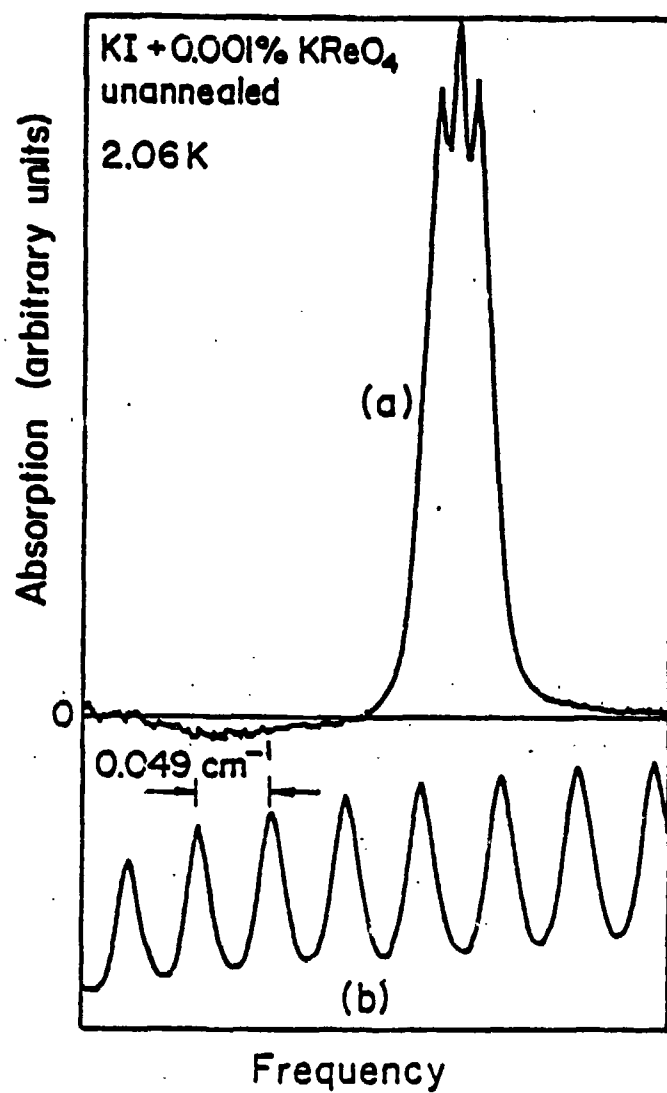


Figure 3. (a) Diode laser absorption spectrum of unannealed KI + 0.001% KReO<sub>4</sub> at 2.06°K. The sample length is 0.2 cm. (b) The etalon trace provides the relative frequency scale near the  $\nu_3$  mode.

structure is not yet known but the sharpness of the triplet structure indicates that well defined quantum states occur even in strained crystals.

## 2. Coincidences with CO<sub>2</sub> laser lines

The diode laser experiments described in the last section demonstrate that CO<sub>2</sub> laser line coincidences with ReO<sub>4</sub><sup>-</sup> modes are expected to be rare in pure alkali halide hosts at low temperatures. Figure 4 schematically shows what happens to the v<sub>3</sub> mode infrared absorption of pure KI:ReO<sub>4</sub><sup>-</sup> as a sample is cooled from 300°K to 1.2°K. The linewidth drops dramatically from a value on the order of 1 cm<sup>-1</sup> at room temperature to roughly 0.02 cm<sup>-1</sup> at helium temperatures. In addition, the v<sub>3</sub> center frequency moves towards higher frequencies due to lattice contraction. The CO<sub>2</sub> laser lines are spaced by 2 cm<sup>-1</sup> and are roughly 1 MHz in width, thus, the probability of the ReO<sub>4</sub><sup>-</sup> v<sub>3</sub> absorption coinciding with any CO<sub>2</sub> laser line at liquid helium temperatures is extremely small. The early progress of this research was impeded by the lack of useable coincident systems. The solution to this problem was to double dope the alkali halide during growth. The second dopant caused an extreme inhomogeneous broadening of the ReO<sub>4</sub><sup>-</sup> v<sub>3</sub> mode absorption with a linewidth of roughly 2 - 3 cm<sup>-1</sup>. The P(42) laser line interacts with KI-RbI (for example) in a region of nearly smooth continuous absorption. By contrast, in KI-CsI:ReO<sub>4</sub><sup>-</sup>, see Figure 4b, the P(42) CO<sub>2</sub> laser line interacts with a split off sideband of unknown origin on the side of a huge v<sub>3</sub> mode central line.

Table 1 summarizes the ReO<sub>4</sub><sup>-</sup> - alkali halide systems known to date to have nonzero absorption on CO<sub>2</sub> laser lines at low temperatures.<sup>6</sup> All of the coincidences listed in this table are unaffected by annealing, with the exception of KBr-LiBr and perhaps KI-LiI. It should be noted that

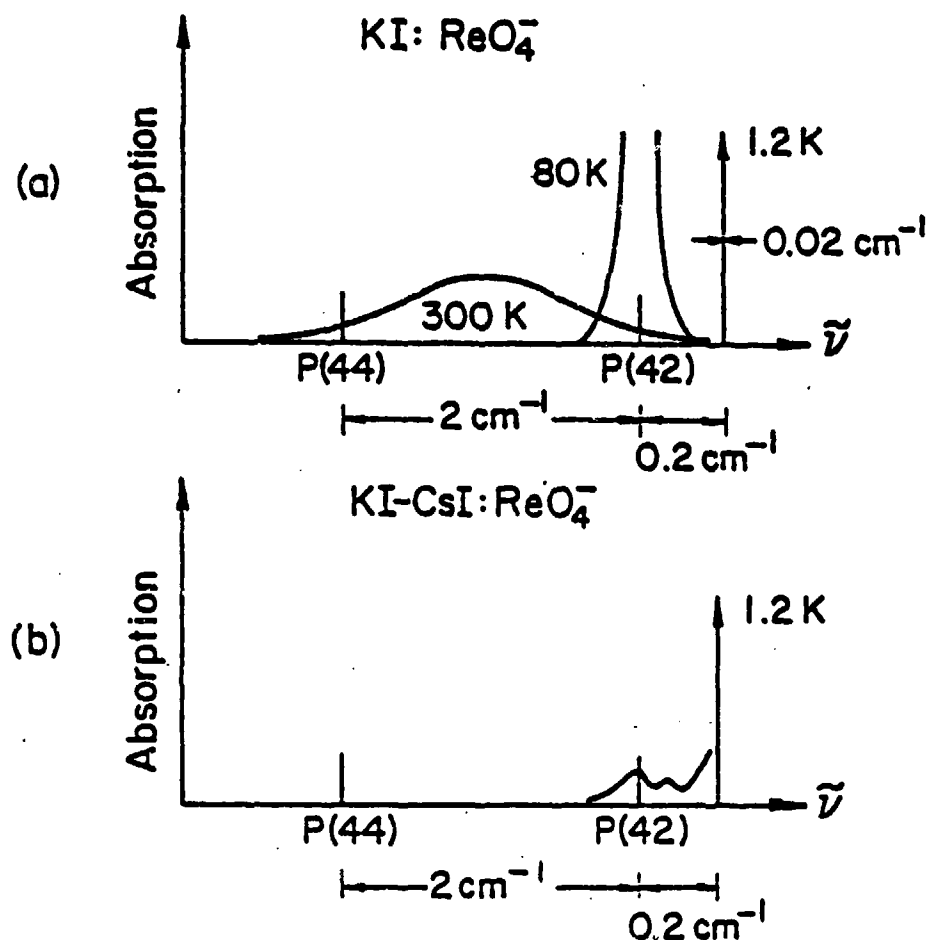


Figure 4. (a) Sketch of temperature dependent absorption lineshape for KI:ReO<sub>4</sub><sup>-</sup>. The positions of the P(44) and P(42) CO<sub>2</sub> laser lines are indicated (10  $\mu\text{m}$  branch). The horizontal axes are not to scale. (b) Sketch of low temperature overlap with P(42) achieved in KI-CsI:ReO<sub>4</sub><sup>-</sup>.

laser line coincidences have been observed in pure Rb salt systems. The detailed explanation for these coincidences is unknown. In some sense, the Rb salts possess a built-in inhomogeneous broadening, because the homogeneous widths of the  $v_3$  mode absorption are as narrow or narrower than in the potassium salts.

### 3. Incoherent saturation

The low temperature saturation properties of the  $\text{ReO}_4^-$   $v_3$  mode have been made in a variety of alkali halides. The experiments have been performed in the so-called incoherent regime, in which the laser pulse length is always much greater than  $T_1$ , the excited state decay time, and  $T_2$ , the excited state dephasing time. The  $v_3$  vibrational mode in alkali halides is inhomogeneously broadened at low temperatures, hence these measurements of  $I_S$ , the saturation intensity or saturation parameter, provide values for the product  $T_1 T_2$  of the two-level system relaxation times. The values of the  $T_1 T_2$  product thus obtained can be combined with values of  $T_2$  from the next section to yield values of  $T_1$  alone.

One particularly advantageous feature of the alkali halides as host lattices is the wide range of phonon frequencies available. If a phenomenon can be observed in a number of these hosts, the effects of changing the lattice phonon spectrum can be obtained. Table 1 shows  $\text{CO}_2$  laser line coincidences of the  $v_3$  vibrational mode of  $\text{ReO}_4^-$  in a variety of potassium, rubidium, and sodium salts. Of particular interest then are the values of  $I_S$  for each of these systems at low temperatures.

Table 2 lists the results of laser saturation studies of  $\text{ReO}_4^-$  molecules in alkali halide lattices at  $1.4^\circ\text{K}$ .<sup>6</sup> These values of  $I_S$ , the saturation parameter,  $\alpha_n$ , the nonsaturable loss and  $T_1 T_2$  have been

Table 1

$\text{ReO}_4^-$  - alkali halide systems with  $\text{CO}_2$  laser line coincidences at 1.4 K

<u>Composition</u>	<u>1.4 K Coincidences</u>	<u>Approximate <math>a(\text{cm}^{-1})</math></u>
KI + 0.05% $\text{KReO}_4$ + 0.2% CsI	P(42)	7
KI + 0.005% $\text{KReO}_4$ + 2.5% RbI	P(42) P(40)	3.5 weak
KI + 0.05% $\text{KReO}_4$ + 2% NaI	P(42)	11.5
KI + 0.2% $\text{KReO}_4$ + 0.05% AgI	P(42)	line 100% deep
KI + 0.2% $\text{KReO}_4$ + 0.2% LiI	P(42)	line 100% deep
	[P(10), P(12)] <sup>a</sup> [P(18), P(30)] <sup>a</sup>	--
KBr + 0.3% $\text{KReO}_4$ + 2.5% RbBr	P(34) P(32)	2.3 $\sim 2$
KBr + 0.2% $\text{KReO}_4$ + 0.2% LiBr	[P(4), P(6), P(8)] <sup>a</sup>	--
KCl + 0.3% $\text{KReO}_4$ + 2.2% RbCl	P(26)	0.1
RbI + 0.8% $\text{KReO}_4$	P(42) P(44)	3 line 100% deep
RbI + 0.02% $\text{KReO}_4$ + 2% KI	P(42) P(44)	1.4 line 100% deep
RbI + 0.4% $\text{RbReO}_4$	P(42)	1.4
RbI + 0.05% $\text{KReO}_4$	P(44)	line 100% deep
RbBr + 0.05% $\text{KReO}_4$	P(38)	2
RbCl + 0.1% $\text{KReO}_4$	P(32)	9
NaI + 0.2% $\text{KReO}_4$	P(26)	5
CsI + 0.05% $\text{KReO}_4$	P(6) P(10) P(44)	2.5 5 weak

<sup>a</sup>Annealed samples of this composition were not studied. Since the room temperature spectra of this sample changed dramatically upon annealing, the existence of these coincidences in annealed samples is yet to be confirmed.

Table 2

Saturation Data for  $\text{ReO}_4^-$  Molecules in Alkali Halides at 1.4 K

Host	Mole % $\text{ReO}_4^-$	Mole % Other	$\tilde{\nu}_3$ (cm $^{-1}$ )	Type <sup>a</sup>	$I_s$ (W/cm $^2$ )	$\alpha_n$ (cm $^{-1}$ ) <sup>b</sup> ( $\pm 25\%$ )	$T_1 T_2$ (10 $^{-16}$ sec $^2$ )
RbI	0.8	0.8 $\text{K}^+$	923 P(42)	A	0.93 $\pm$ 0.2	0.90	24 $\pm$ 5
				UA	0.87 $\pm$ 0.2	0.21	28 $\pm$ 6
KI	0.005	2.5 $\text{Rb}^+$	923 P(42)	A	3.6 $\pm$ 0.8	0.13	6.7 $\pm$ 1.5
				UA	0.75 $\pm$ 0.2	0.10	31 $\pm$ 10
KI	0.05	2.0 $\text{Na}^+$	923 P(42)	A	3.2 $\pm$ 0.6	0.12	7.6 $\pm$ 1.5
				UA	3.6 $\pm$ 0.7	0.08	6.7 $\pm$ 1.3
KI	0.05	0.2 $\text{Cs}^+$	923 P(42)	A	6.8 $\pm$ 1.4	0.55	3.6 $\pm$ 0.8
				UA	3.9 $\pm$ 0.8	2.8 <sup>s</sup>	6.1 $\pm$ 1.3
RbBr	0.05	0.05 $\text{K}^+$	927 P(38)	A	14 $\pm$ 3	1.1	1.8 $\pm$ 0.4
				UA	19 $\pm$ 4	0.30	1.4 $\pm$ 0.3
KBr	0.3	2.5 $\text{Rb}^+$	931 P(34)	A	53 $\pm$ 10	0.41	0.49 $\pm$ 0.09
				UA	59 $\pm$ 12	0.10	0.42 $\pm$ 0.09
RbCl	0.1	0.1 $\text{K}^+$	933 P(32)	A	9.3 $\pm$ 2	1.4	2.9 $\pm$ 0.6
				UA	9.6 $\pm$ 2	1.2	2.8 $\pm$ 0.6
NaI	0.2	0.2 $\text{K}^+$	939 P(26)	UA	>700	--	<0.05
KCl	0.3	2.2 $\text{Rb}^+$	939 P(26)	UA	22 $\pm$ 5	0.1	1.2 $\pm$ 0.3

<sup>a</sup>UA - unannealed sample, A - sample annealed 2 hours in air

<sup>b</sup>Varies, depending on location in boule

extracted from the inhomogeneous saturation curves similar to Figure 1. For most of the hosts, the saturation intensity for the unannealed samples is similar to that for the annealed samples.

The values of the saturation parameter,  $I_s$ , are equivalent to measurements of the inverse excited state life time. This follows because the results of the next section show that  $T_2$  is roughly  $2 T_1$  at 1.4°K i.e. the molecular dephasing is being determined by excited state decay. Since  $T_1 T_2$  does not really contain two independent parameters, the variation of  $I_s$  with host parameters can be viewed as a variation of the excited state decay rate squared.

The study of the alkali halide dependence of the  $\nu_3$  excited state decay rate suggests that a combination of molecular internal modes, local modes of the lattice-impurity complex, and band phonons represents the dominant decay channel, rather than the previously expected multiphonon decay.

Figure 5 diagrams the expected decay process for the various alkali halide hosts. In all cases, two internal modes of the  $\text{ReO}_4^-$  molecule are excited. The remaining energy mismatch between  $\nu_3$  and  $2\nu_4$  or  $(\nu_4 + \nu_2)$  is provided by localized and extended phonon excitations. In KI, KBr, RbBr and RbI, the energy mismatch is provided by the excitation of an even local mode and one band mode (Figure 5a). However, the extremely large value of  $I_s$  in NaI indicates that the local mode frequency is large enough to account for the mismatch by itself--no band phonons are required (Figure 5b). (The local mode in NaI occurs at a higher frequency than in the other hosts because it involves the motion of the lighter  $\text{Na}^+$  ion). In the RbCl case, the local mode occurs in the gap and is of much lower

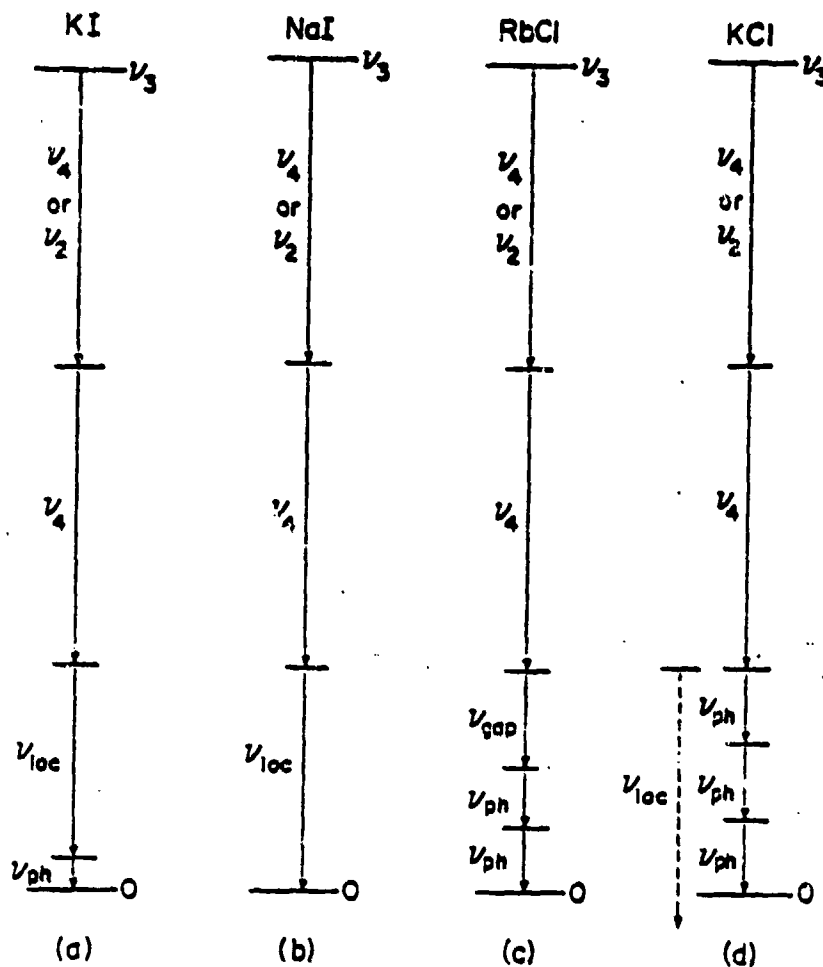


**Figure 5.** Multistep anharmonic decay process for the  $v_3$  mode of  $\text{ReO}_4^-$  in alkali halides. (a) In KI, the energy of the  $v_3$  mode produces two internal mode excitations,  $v_2 + v_4$  or  $2v_4$ , a local mode excitation, and a band phonon. (b) In NaI, the local mode frequency has grown to the extent that no additional band phonon is required to achieve energy conservation. (c) In RbCl, the local mode occurs at lower frequency than in the other cases because it appears in the gap in the phonon spectrum. Hence two band phonons are required to achieve energy conservation. (d) In KCl, the frequency of the local mode is so large that a local mode excitation cannot be used to de-excite the  $v_3$  mode. Three band phonons are required to complete the decay.

frequency, hence two phonon modes are required to conserve energy (Figure 5c). Finally for KCl (Figure 5f) the local mode is of such high frequency that it cannot participate in the decay process at all. Thus the anomalies in  $I_5$  occur because the  $v_3$  mode decay process is third order in NaI, 5th order in RbCl and KCl and fourth order in all the other hosts.

#### 4. IR hole burning

Incoherent saturation measurements such as those described in the last section can only measure the product  $T_1 T_2$  for inhomogeneously broadened lines at low temperatures. In order to study the relaxation times  $T_1$  and  $T_2$  separately, one or the other must be measured independently. The technique of hole burning spectroscopy allows measurement of the homogeneous linewidth (and thus  $T_2$ ) inside an inhomogeneously broadened absorption line. Briefly, a pump laser at  $\omega_0$  partially saturates absorbers with center frequency near  $\omega_0$ , and a tuneable low-power probe laser measures the frequency-dependent decrease in absorption (the "hole") for these systems. The homogeneous linewidth and the homogeneous dephasing time,  $T_2$ , can be extracted from the hole lineshape.

Using diode laser-CO<sub>2</sub> laser hole burning spectroscopy<sup>8</sup> we have been able to measure the temperature-dependent homogeneous dephasing time  $T_2$  of the ReO<sub>4</sub><sup>-</sup>  $v_3$  mode in crystalline alkali halides.

Figure 6 shows the homogeneous linewidth<sup>8</sup> of the ReO<sub>4</sub><sup>-</sup>  $v_3$  mode over the temperature range 1.4 - 600°K. The hole burning 25°K due to the rapid increase of  $I_5$  and consequent decrease in hole depth with increasing temperature. Note that the data for the pure KI and the alloy hosts connect continuously at 25°K. Further, the homogeneous linewidths

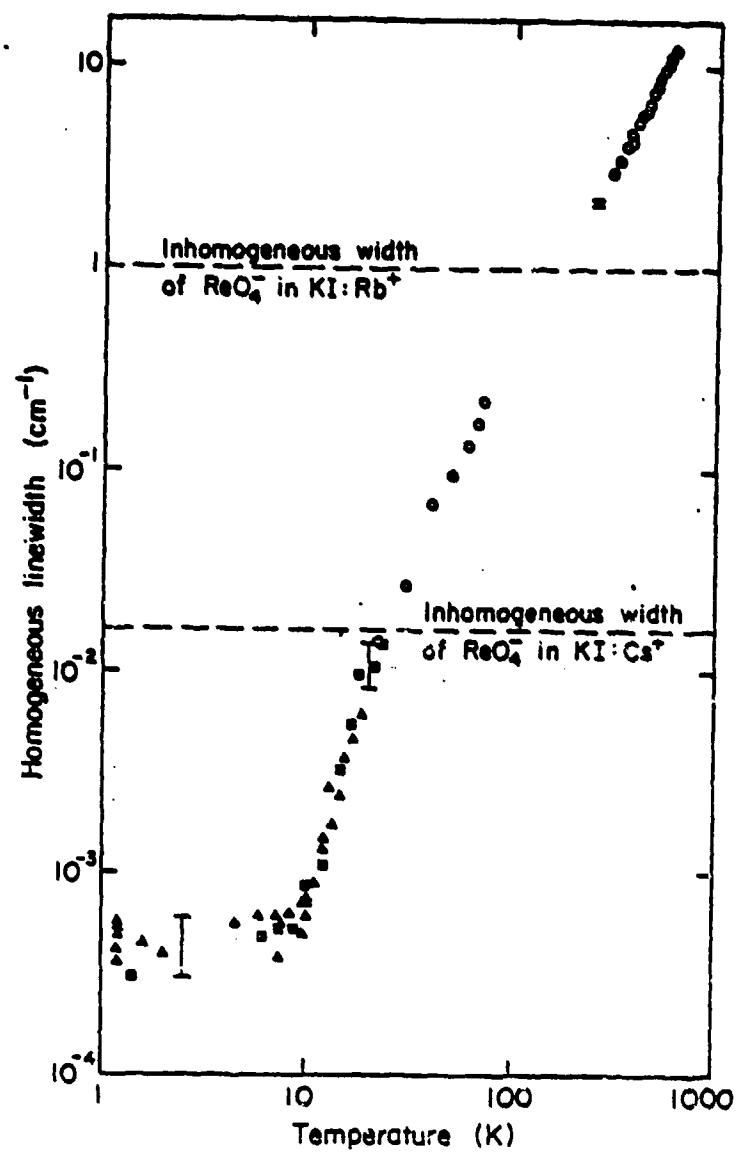


**Figure 6.** Homogeneous linewidth (FWHM) of the  $\nu_3$  vibration of  $\text{ReO}_4^-$  in KI crystals versus temperature. The open circles represent the linear spectroscopic measurements described in Section 1. The squares represent hole burning results for samples of composition KI + 0.005% KReO<sub>4</sub> + 2.5% RbI, and the triangles represent equivalent data for KI + 0.05% KReO<sub>4</sub> + 0.2% CsI samples. The inhomogeneous linewidths for these two hosts are indicated.

are essentially equal for the two alloy hosts despite the large difference in homogeneous widths. This indicates that the hole widths are determined by the lattice phonons of the host lattice rather than the detailed nature of the second dopant. A detailed theoretical fit to the experimental data over four orders of magnitude confirm the identification of acoustic phonons as the excitations primarily responsible for the dephasing of the  $v_3$  mode above 10°K.

For ultra narrow spectral lines a convenient way to conduct hole burning experiments without a diode laser is to use two CO<sub>2</sub> lasers--one for the fixed frequency pump and the other for the tuneable probe. The oscillation frequency of a 1 m CO<sub>2</sub> laser can be tuned over roughly  $\pm$  40 MHz simply by varying the cavity length with a piezoelectric transducer. The use of a CO<sub>2</sub> laser as the tuneable probe has several advantages over the semiconductor diode laser. The CO<sub>2</sub> laser automatically tunes above and below every CO<sub>2</sub> laser line, so that the problem of finding a diode laser that lases at a specific CO<sub>2</sub> frequency has disappeared. This means that almost all ReO<sub>4</sub><sup>-</sup> - alkali halide systems with CO<sub>2</sub> laser line coincidences can be studied with ease. Furthermore, the frequency jitter of the CO<sub>2</sub> laser is five times smaller than the jitter of the diode laser, allowing hole burning measurements at much higher resolution. The principal disadvantage of the CO<sub>2</sub> probe is its limited tuning range; broad holes greater than ~ 70 MHz in width cannot be studied. The low temperature (1.4 K) homogeneous linewidths of the ReO<sub>4</sub><sup>-</sup>  $v_3$  mode in most alkali halides are small enough that this restricted tuning range presents no serious problem (fortunately).

Table 3 summarizes the results of the CO<sub>2</sub>-CO<sub>2</sub> hole burning

Table 3

Homogeneous Linewidths,  $T_2$ , and  $T_1$  for  $\text{ReO}_4^-$  in Alkali Halides at 1.4 K

Host	Mole % $\text{ReO}_4^-$	Mole % Other	$\tilde{\nu}_3(\text{cm}^{-1})$	$\Delta\nu_{\text{HOLE}}$ (MHz)	$\Delta\nu_{\text{HOM}}$ (MHz)	$T_2$ ( $10^{-8}$ sec)	$T_1$ ( $10^{-8}$ sec)
RbI	0.8	$0.8 \text{ K}^+$	923 P(42)	10 $\pm$ 3	5.0 $\pm$ 1.5	6.4 $\pm$ 2.0	3.8 $\pm$ 1.4
				11 $\pm$ 3	5.5 $\pm$ 1.5	5.8 $\pm$ 1.6	-
				9 $\pm$ 2.5	4.5 $\pm$ 1.5	7.1 $\pm$ 2.4	3.9 $\pm$ 1.4
KI	0.05	$2.5 \text{ Rb}^+$	923 P(42)	15.5 $\pm$ 1	7.8 $\pm$ 0.5	4.1 $\pm$ 0.3	1.6 $\pm$ 0.5
				15 $\pm$ 1	7.5 $\pm$ 0.5	4.2 $\pm$ 0.3	7.4 $\pm$ 0.5
KI	0.05	$0.2 \text{ Cs}^+$	925 P(40)	29 $\pm$ 2	14.5 $\pm$ 1	2.2 $\pm$ 0.2	-
				18 $\pm$ 2.5	9.0 $\pm$ 1.3	3.5 $\pm$ 0.5	1.0 $\pm$ 0.3
KI	0.05	$2.0 \text{ Na}^+$	923 P(42)	16 $\pm$ 1	8.0 $\pm$ 0.5	4.0 $\pm$ 0.3	1.5 $\pm$ 0.4
				20 $\pm$ 3	10 $\pm$ 1.5	3.2 $\pm$ 0.5	2.4 $\pm$ 0.5
KI	0.2	$0.2 \text{ Li}^+$	923 P(42)	15 $\pm$ 2	7.5 $\pm$ 1	4.2 $\pm$ 0.6	1.6 $\pm$ 0.6
				19 $\pm$ 2	9.5 $\pm$ 1	3.4 $\pm$ 0.4	-
RbBr	0.05	$0.05 \text{ K}^+$	927 P(38)	36 $\pm$ 3	18 $\pm$ 1.5	1.8 $\pm$ 0.2	1.0 $\pm$ 0.3
				45 $\pm$ 4	23 $\pm$ 2	1.4 $\pm$ 0.1	1.0 $\pm$ 0.3
KBr	0.3	$2.5 \text{ Rb}^+$	931 P(34)	60 $\pm$ 3	30 $\pm$ 1.5	1.1 $\pm$ 0.1	0.45 $\pm$ 0.15
RbCl	0.1	$0.1 \text{ K}^+$	933 P(32)	34 $\pm$ 2.5	17 $\pm$ 1.3	1.9 $\pm$ 0.2	1.5 $\pm$ 0.3
				33 $\pm$ 2.5	17 $\pm$ 1.8	1.9 $\pm$ 0.2	

measurements<sup>6,9</sup> of the homogeneous linewidth at 1.4°K.  $T_2$  is computed from the homogeneous width.  $T_1$  is derived from  $T_2$  and the values of the  $T_1 T_2$  product, represented in Table 1. Due to the high saturation parameter and low absorption, respectively, hole spectra could not be obtained for the NaI and KCl hosts.

Inspection of the table shows that for all samples, the hole width is essentially independent of sample annealing. Furthermore, the  $T_2$  values for the various KI hosts do not depend strongly on the second cation dopant. Thus, the hypothesis that the addition of the second dopant does not strongly change the microscopic relaxation channels for the  $v_3$  vibrational mode is verified. This is a happy consequence, because double doping was essential in order to produce CO<sub>2</sub> laser line coincidences.

Comparison of the  $T_1$  and  $T_2$  values for the various hosts in Table 3 leads to an important conclusion. Within experimental error, the data for the annealed samples obey the relation  $1 < T_2/T_1 < 2$ . This is conclusive evidence that the dephasing of the  $v_3$  mode is dominated by excited state decay. In this limit, saturation measurements can be viewed as measuring a single independent quantity, the excited state decay rate (squared) rather than the product of two independent quantities, the decay rate and dephasing rate. Thus, the analysis of the ReO<sub>4</sub><sup>-</sup> decay channel using measurements of  $I_S$  is valid.

##### 5. The persistent hole

Figure 7a shows the growth and detection of a persistent spectral hole<sup>10</sup> in RbI:ReO<sub>4</sub><sup>-</sup> using a single CO<sub>2</sub> laser (called the probe). The vertical axis in the figure gives the transmission of the sample at the 10.8 μm P(42) laser line. After cooling to 1.4 K in the dark, the probe

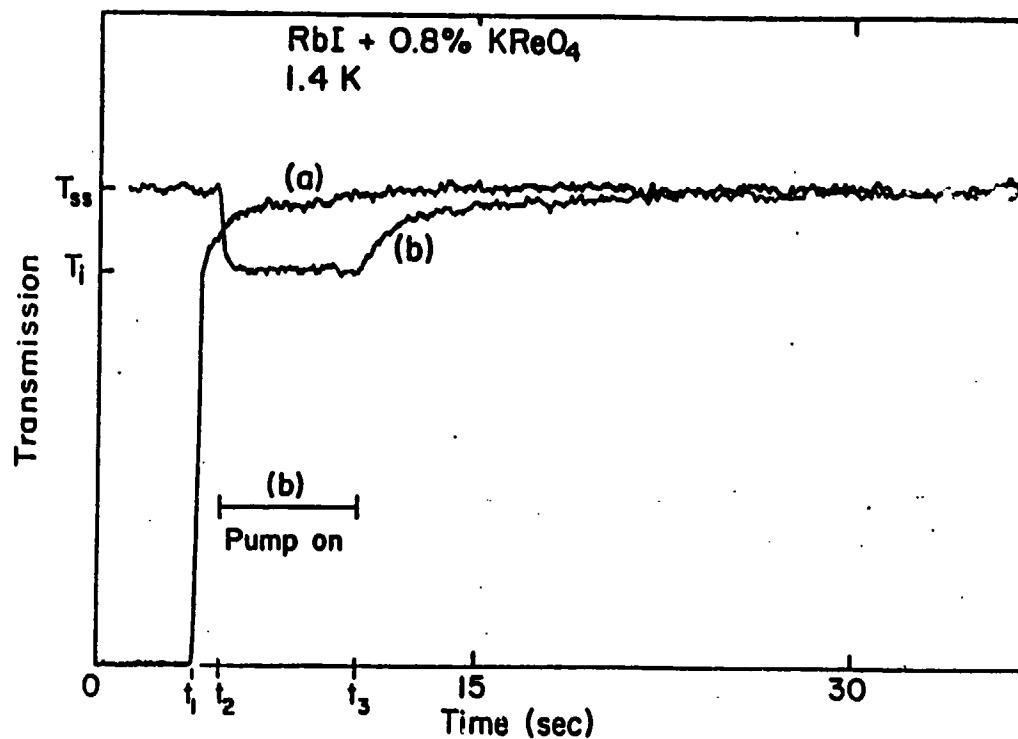


**Figure 7.** Examples of long-lived hole growth and erasing observed by direct detection methods. (a) After cooling the sample from 77 K to 1.4 K in the dark, the probe beam is unblocked at time  $t_1$ . The probe transmission increases very slowly over many seconds, indicating the growth of a hole burned by the probe. The initial transmission just after unblocking is  $T_i$ , and the steady-state transmission is  $T_{ss}$ . The absolute value of  $T_i$  is 0.02. (b) After long exposure to the probe beam, the pump is unblocked at time  $t_2$ , erasing the probe hole, and blocked again at time  $t_3$ . The difference frequency between pump and probe is 10 MHz.

laser is unblocked at time  $t_1$ . The sample transmission quickly jumps to an initial value  $T_i$ , and then slowly grows over many seconds to a steady state value,  $T_{ss}$ . This is line-center detection of the hole in which the same laser beam acts as both a burning and probing laser. The fractional hole depth saturates at a value in the range 0.05 - 0.3, independent of laser power. The hole growth is non-exponential, showing a fast growth rate at small times and a slow rate at large times and these rates scale with laser power, high power giving faster approach to the steady state depth.

The hole lifetime is extremely long: the probe laser beam can be blocked for times as long as 10 minutes after the transmission has reached  $T_{ss}$ , and subsequent unblocking shows an immediate jump of the transmission to the values  $T_{ss}$ . Longer dark times could not be studied due to laser frequency drift.

A second CO<sub>2</sub> laser beam (called the pump) can be used to erase the hole burned by the probe. Figure 7b shows how the probe transmission drops from  $T_{ss}$  to approximately  $T_i$  when the pump laser is allowed to irradiate the sample from time  $t_2$  to  $t_3$ . In the case, the frequency separation between pump and probe,  $\Delta f$ , is 10 MHz. The efficiency of hole erasing is zero at  $\Delta f = 0$  MHz, grows to a maximum of 100% for  $\Delta f = 10 - 15$  MHz (for  $I_{\text{pump}}/I_{\text{probe}} > 350$ ), and falls off to 50% at  $\Delta f = 30$  MHz.

At the P(42) the absorption coefficient change caused by the hole  $\Delta\alpha$ , is linear in the total absorption in the absence of the hole,  $\alpha_i$ . This suggests that single, isolated ReO<sub>4</sub><sup>-</sup> molecules are responsible for the HB process. Furthermore, the effective growth rate (assuming a single exponential for convenience only) depends linearly upon the burning beam

intensity, implying that HB occurs via a one-photon process. The burning efficiency, defined as the number of centers losing absorption at the laser frequency divided by the number of photons absorbed is in the range  $10^{-3}$  to  $10^{-4}$ . This compares to values of  $10^{-6}$  -  $10^{-7}$  for color centers and photostable molecules in glasses.

A natural configuration for the  $\text{ReO}_4^-$  substituted for the halide ion in an alkali halide crystal is with the four tetrahedral Re-O bonds directed in four of the eight available  $\langle 111 \rangle$  directions. The molecular ion has as a consequence two possible configurations denoted A and B depending upon which choice is made for the bond directions. These two configurations may be expected to be different in energy by an amount, denoted  $\epsilon$  in Figure 8, proportional to an appropriate component of the elastic strain gradient due to nearby defects. The upper wells correspond to excitation of the  $\hbar\omega_3$  vibration, and because of the different vibrational state, the strain induced inequivalence is assumed different from that in the ground state by an amount  $\Delta \equiv \epsilon^* - \epsilon$ . The importance of the strain induced inequivalence is suggested by the observation that persistent holes are only observed in the wings of the inhomogeneous broadened line, corresponding to sites of large local strain. The levels in each of the local wells are to indicate possible excitation of librational modes of the  $\text{ReO}_4^-$  about the equilibrium configurations in any of the three distinct degenerate coordinates which, because of the equivalence of the four oxygen ions, can take the system from A to B. Tunneling is supposed too weak to allow reorientation, in the librational ground state, from A to B, at the temperature, 1.4 K, of these experiments, and is also assumed small compared with  $\epsilon$ .

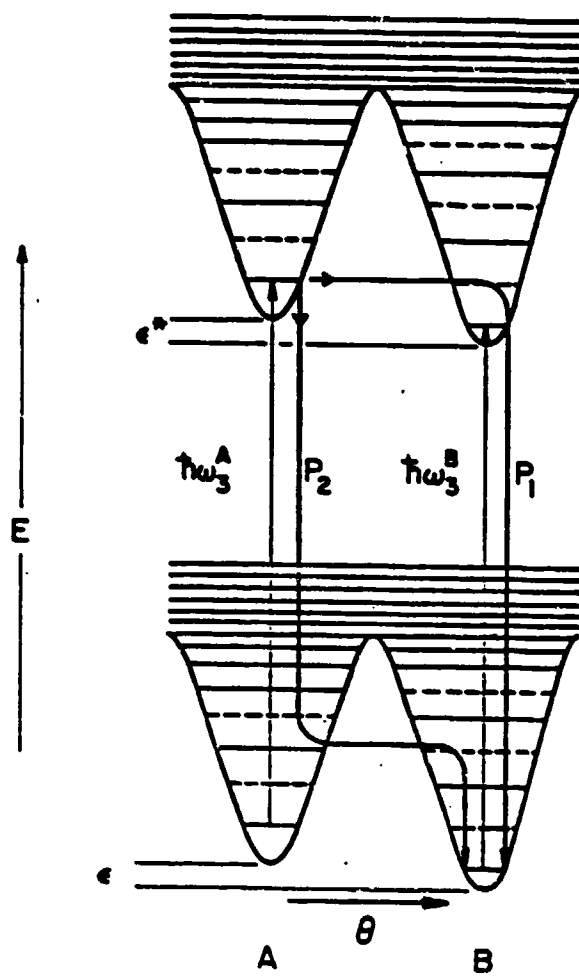


**Figure 8.** Potential energy diagrams for the spherical top molecule in the ground and excited vibrational states. Two possible configurations denoted by A and B occur for each state. Librational states occur near the bottom of the wells and free rotor states at energies above the potential barrier. The solid lines in a particular well are to indicate that the probability amplitude is localized there. The molecular reorientation coordinate is denoted by  $\theta$  and  $P_1$  and  $P_2$  show two possible decay paths which produce molecular reorientation.

Our observation and interpretation of persistent spectral holes in the vibrational mode of a spherical top molecule embedded in a cubic site of alkali halide lattice complement the earlier studies on electronic transitions in organic glasses. We conclude that persistent nonphotochemical hole burning at low laser intensity is a general solid state phenomena which can occur whenever the complete ground state of the system to be excited has configurational degeneracy.

### C. Paraelectric Centers in Li Doped Alkali Halides Crystals

A number of defect-host combinations produce isolated electric dipoles in alkali halide crystals.<sup>12</sup> The impurities divide naturally into two groups: (1) those which have intrinsic dipoles such as OH<sup>-</sup>, CN<sup>-</sup> or NO<sub>2</sub><sup>-</sup> and (2) those in which the defect host combination itself produces an effective dipole such as for Li<sup>+</sup> in KCl, F<sup>-</sup> in NaBr or Ag<sup>+</sup> in RbCl.

Some lattice-defect combinations have been discovered which contain resonances near zero frequency but do not possess a permanent moment as for the off-center ions described above. Examples are KBr:Li<sup>+</sup>, NaI:Cl<sup>-</sup>, NaCl:Cu<sup>+</sup>, NaCl:Ag<sup>+</sup> and KI:Ag<sup>+</sup>.

All of these low frequency infrared active modes are extremely anharmonic and can be tuned over 100% with hydrostatic pressure. The tunneling modes have the additional feature that they can be tuned over a similar frequency range with uniaxial stress or an applied electric field.

It is known that Li<sup>+</sup> in KBr produces a resonant mode at 16 cm<sup>-1</sup> while Li<sup>+</sup> in KCl produces a tunneling mode at 1 cm<sup>-1</sup>. Also ReO<sub>4</sub><sup>-</sup> in KBr and KCl is known to strain the local lattice because of the large diameter of the molecule. Double doping KBr with Li<sup>+</sup> and ReO<sub>4</sub><sup>-</sup> relaxes the local lattice somewhat and produces correlated impurity pairs. A low concentration of Li<sup>+</sup> impurities produces two sidebands on the ReO<sub>4</sub><sup>-</sup> internal mode. Increasing Li<sup>+</sup> concentration simply increases the two sidebands at the expense of the central unshifted ReO<sub>4</sub><sup>-</sup> line. Two lines are expected for a Li<sup>+</sup> nearest neighbor to the ReO<sub>4</sub><sup>-</sup> molecule since the cubic symmetry is removed and a singly degenerate and a doubly degenerate mode replace the threefold degenerate v<sub>3</sub> mode.

We have found that Li<sup>+</sup> ions can be diffused into KBr:ReO<sub>4</sub><sup>-</sup>

systems at 600°C. During a Li diffusion experiment we found that a number of absorption lines appeared at frequencies below 6 cm<sup>-1</sup>; and these lines were in addition to the resonant mode at 16 cm<sup>-1</sup>.

More extensive studies have shown that these lines are the same as reported by Bridges<sup>13</sup> using paraelectric resonance techniques. Because these lines tune easily with electric field Bridges has concluded that Li<sup>+</sup> in KBr is a paraelectric system. This interpretation conflicts with the resonant mode model. To clarify the experimental situation we have made a systematic study of millimeter wave properties of the two Li<sup>+</sup> isotopes in KBr.

The experimental results are shown in Figure 11. The top trace indicates that two low frequency lines occur in Li<sup>7</sup> while the bottom trace shows that four lines occur in Li<sup>6</sup>. The clue to the source of these modes is in the center trace where a crystal containing a 50-50 mixture of the two isotopes is displayed. If the lines were associated with isolated impurities then the central trace would only contain the sum of both sets of lines but this is not the case. New strong lines appear at 5.5 cm<sup>-1</sup> and 3.2 cm<sup>-1</sup> for the mixture. This pattern is to be expected if these low frequency lines are associated with Li<sup>+</sup> pairs. In this case 25% of the centers would be associated with Li<sup>6</sup> - Li<sup>6</sup>, 25% with Li<sup>6</sup> - Li<sup>7</sup> and 50% with Li<sup>6</sup> - Li<sup>7</sup> since there are two ways of forming this combination. Because the strongest lines observed are the new combination lines we assign the low frequency spectrum to pairs of ions. The interesting new result is that the isolated Li<sup>+</sup> ions are barely stable on center in KBr but when two Li<sup>+</sup> ions are in neighboring cells the ions are unstable and move off center in a collective manner.

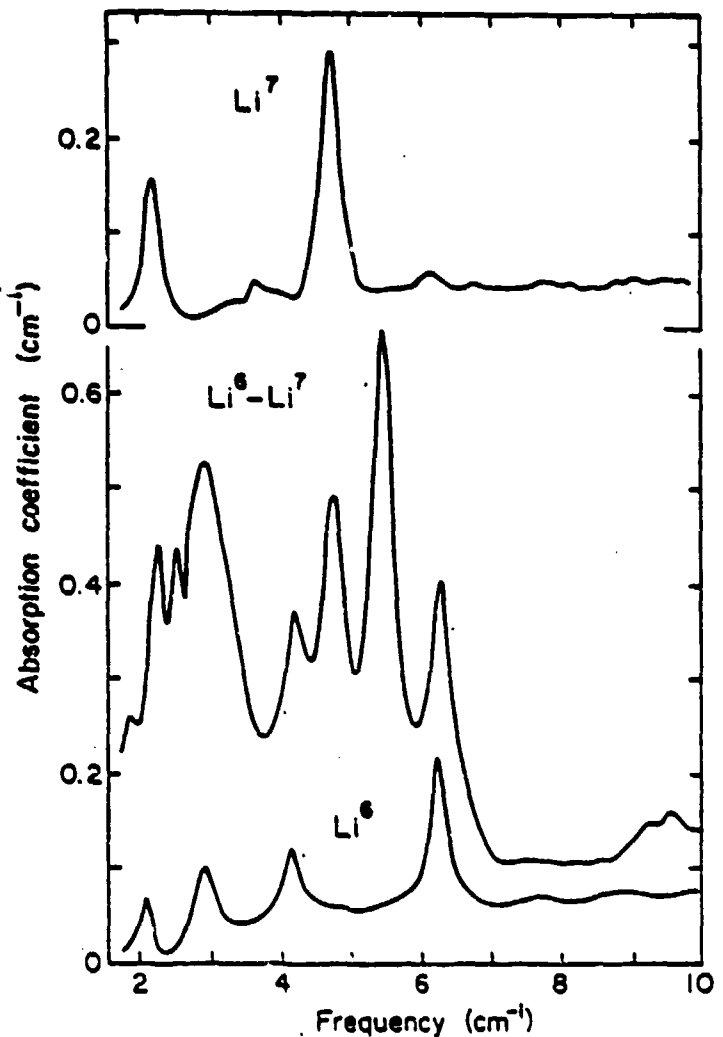


**Figure 11.** Low frequency paraelectric modes of Li in KBr. The top trace shows two absorption lines for  $\text{Li}^7$  and the bottom trace shows four lines for  $\text{Li}^6$ . The central trace shows that these lines are due  $\text{Li}^+$  pairs since a 50-50 mixture of  $\text{Li}^6 - \text{Li}^7$  produces new combination lines.

We have found by diffusion doping that it is possible to produce as many pair centers as isolated centers. It will be interesting to see how these pairs behave when they are in the vicinity of a  $\text{ReO}_4^-$  ion.

D. CO<sub>2</sub> Laser Saturation of Local Modes in CaF<sub>2</sub>:H<sup>-</sup>:Er<sup>3+</sup>

Negative hydride ions can be incorporated into alkaline earth fluoride crystals and these then show infrared absorption due to localized modes of the hydride ion.<sup>14</sup> In alkaline earth fluoride crystals containing trivalent rare earth ions, the hydride ions can serve as charge compensators for the rare earth ions. In calcium fluoride a common form of charge compensation is provided by interstitial hydride ions in an empty fluorine cell adjacent to the trivalent rare earth ion. Both the rare earth ion and the hydride ion possess C<sub>4v</sub> symmetry in this arrangement. The local mode spectrum of the hydride ions consists of two lines in the infrared absorption spectrum. The energy levels for CaF<sub>2</sub>:H<sup>-</sup>:Er<sup>3+</sup> are shown in Figure 12. The lower frequency local mode line with C<sub>4v</sub> symmetry is the doubly degenerate (X,Y) vibration of the hydride ion "transverse" to the rare earth-hydride ion axis. The higher frequency line is the Z vibration of the hydride ion along the rare earth-hydride ion axis. In general the frequencies of these lines vary with the particular rare earth ion and several of them fall within the range of frequencies obtainable from a CO<sub>2</sub> laser. Of these, the X,Y local mode vibrations of calcium fluoride crystals containing dysprosium, holium, erbium, thulium, lutecium and yttrium and the Z local mode vibrations of CaF<sub>2</sub> crystals containing dysprosium, erbium, thalium, ytterbium and lutecium are all accessible to measurement with a CO<sub>2</sub> laser.

In a preliminary study we have observed high intensity infrared laser saturation of the hydride ion local mode absorption lines in calcium fluoride crystals containing erbium. Similar saturation effects were not observed in the corresponding hydrogen local mode lines of dysprosium,

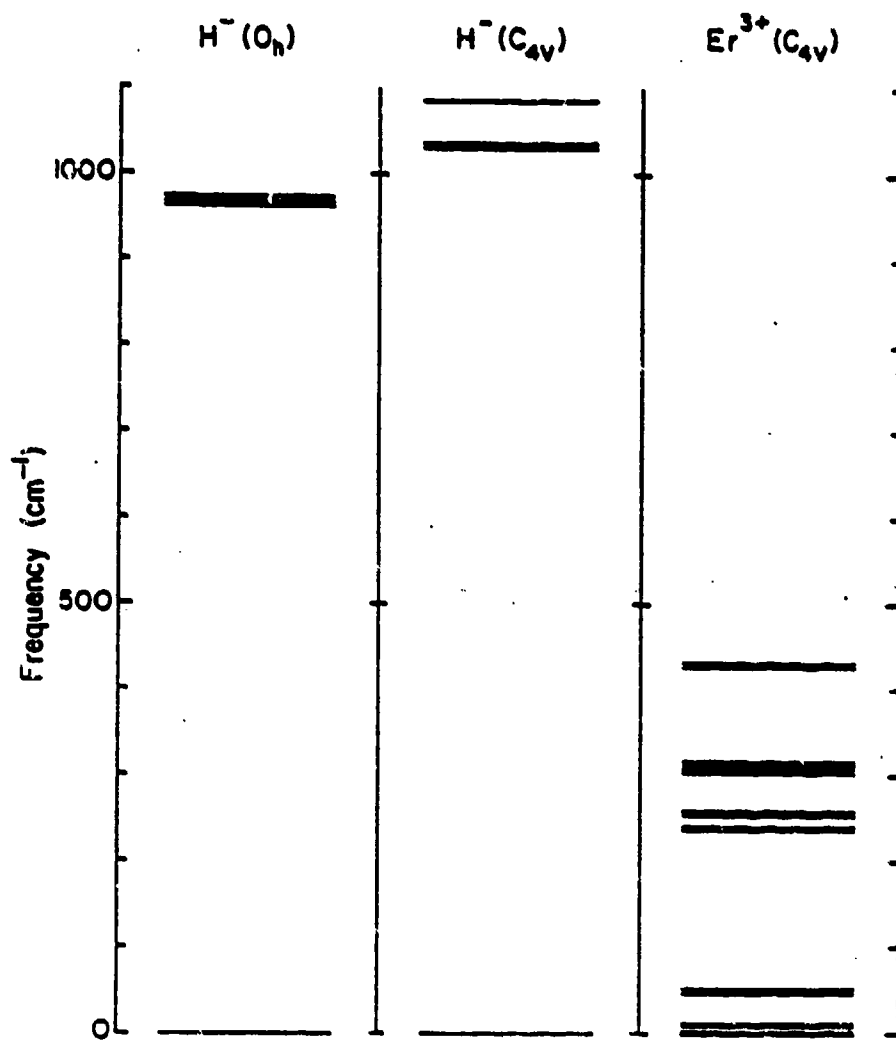
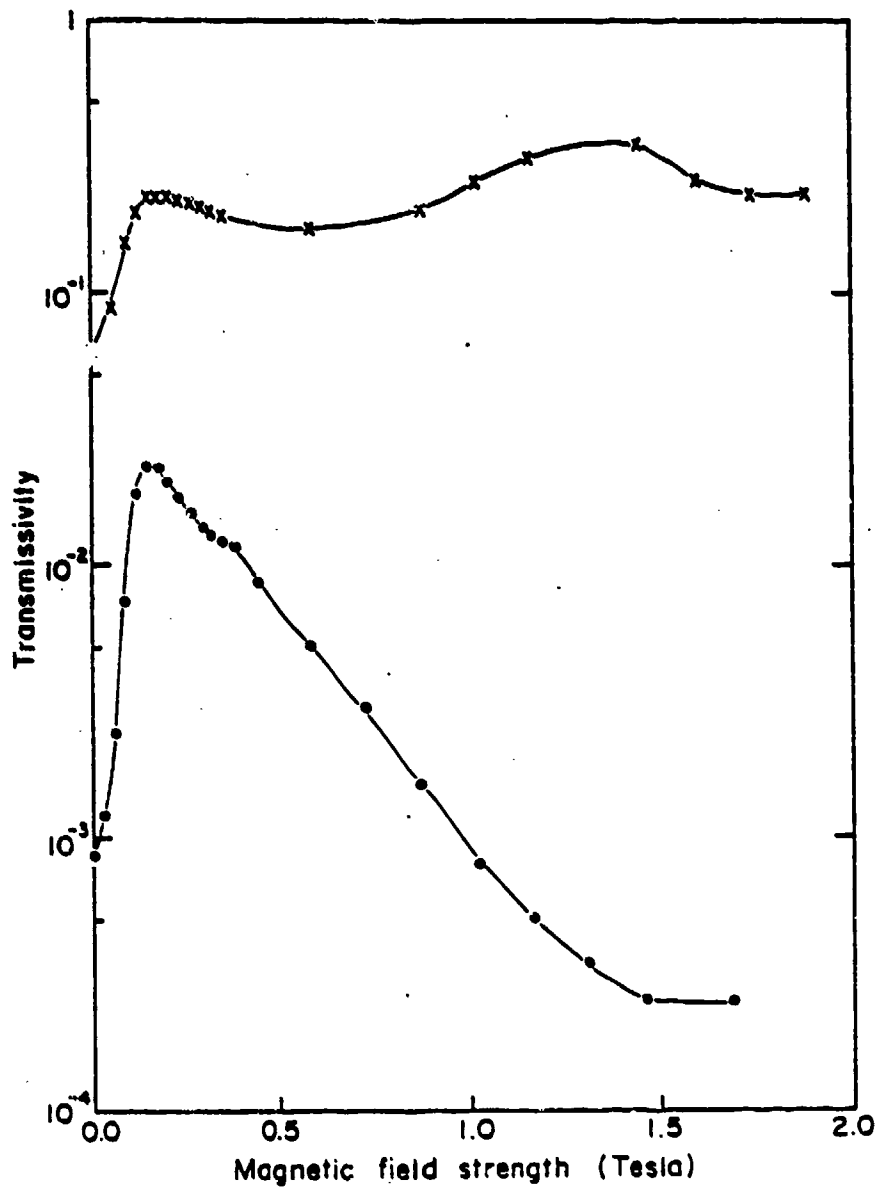


Figure 12. Energy levels of  $H^-$  local modes and  $Er^{3+}$  crystal field levels in  $\text{CaF}_2$ . The vibrational level of isolated  $H^- (O_h)$  can decay by a two phonon process. For correlated  $H^-$ : $Er^{3+}$  pairs both ions have  $C_{4v}$  symmetry. The split  $H^-$  vibrational mode can decay either by a three phonon process or by two  $Er^{3+}$  crystal field transitions plus a one phonon transition.



**Figure 13.** Transmissivity of  $\text{CaF}_2:\text{H}^-:\text{Er}^{3+}$  versus magnetic field for a low and high laser intensity. The high intensity data is at  $100 \text{ KW/cm}^2$ . The sample is at  $2^\circ\text{K}$ .

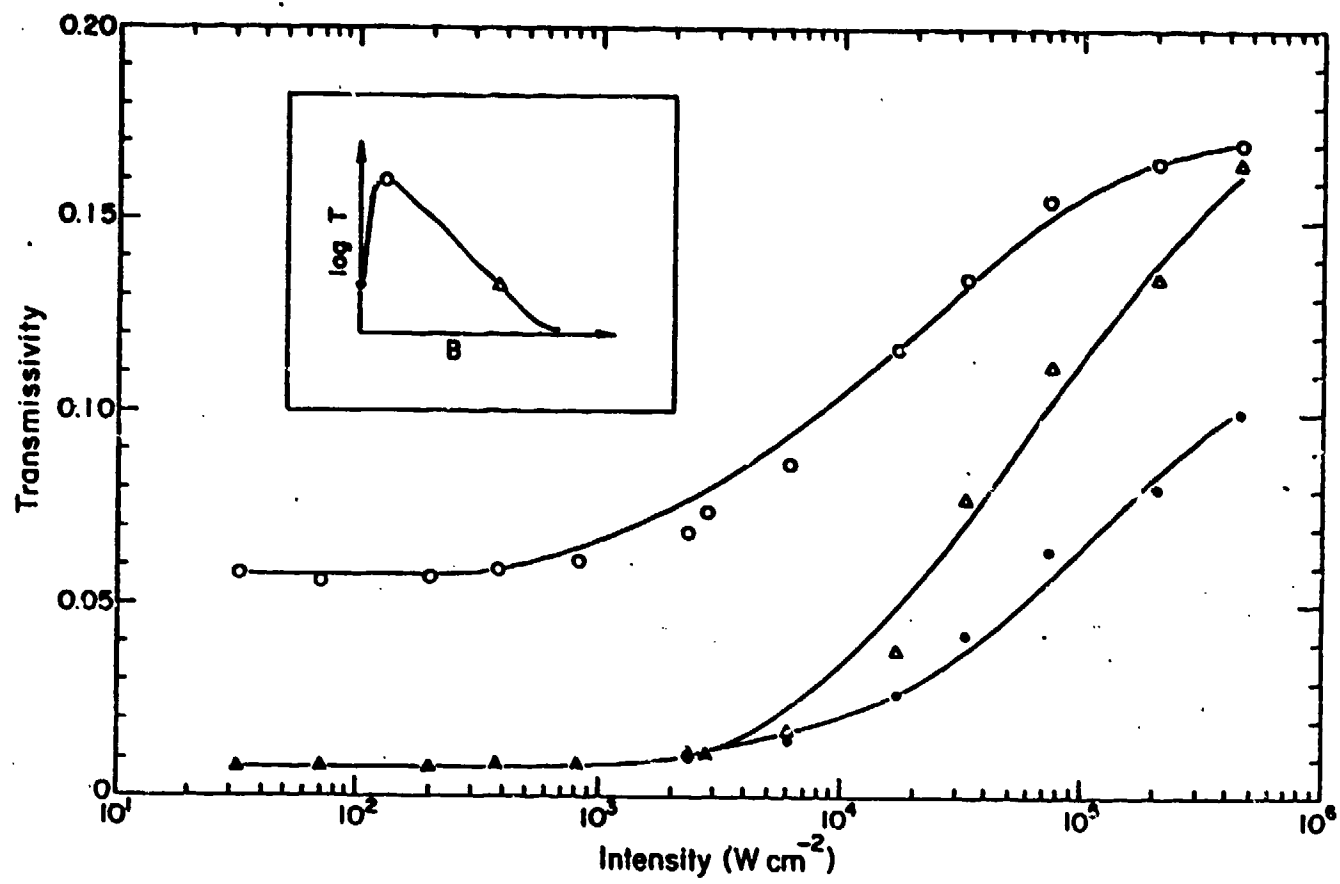


Figure 14. Transmissivity of  $\text{CaF}_2:\text{H}^-:\text{Er}^{3+}$  versus laser intensity for different magnetic fields. The three fields used are shown in the insert which represents the low intensity spectrum in Figure 13.

holmium, thulium, lutecium and yttrium in  $\text{CaF}_2$ .

The transmissivity of  $\text{CaF}_2:\text{H}^-:\text{Er}^{3+}$  versus magnetic field for a low and high laser intensity are shown in Figure 13. The low signal trace shows that a set of magnetic field dependent local mode transitions move out and into coincidence with the  $\text{CO}_2$  laser line. The high intensity data at  $100 \text{ KW/cm}^2$  shows that the local mode lines do indeed saturate and that the saturation parameter depends on magnetic field.

The field dependence of the saturation behaviour can be seen more clearly in Figure 14 where the transmissivity is graphed as a function of laser intensity. The solid lines are fits to the data using an inhomogeneous line broadening model. The saturation parameter is about  $1 \text{ MW/cm}^2$ .

The crystal field levels of erbium ions in the  $\text{C}_{4v}$  site have been determined by optical measurements and the  ${}^4\text{I}_{15/2}$  energy level scheme is presented in Figure 12. A feature of this site in erbium, as compared to other rare earth ions, is the occurrence of a low lying electronic level  $4.5 \text{ cm}^{-1}$  above the ground level. The exact position of this level was measured as  $4.4 \text{ cm}^{-1}$  at  $1.2^\circ\text{K}$  by far infrared absorption measurements on 5 cm long specimens of hydrogenated calcium fluoride crystals containing 0.05% erbium.

The measured magnetic field dependence of the local mode frequency indicates that the erbium crystal field levels are coupled to the hydride ion local mode levels through the electron-local mode phonon interaction. The vibronic states of the erbium ion-hydride system can be represented by linear combinations of product states of the erbium electronic wavefunctions and the X,Y,Z local mode phonon states.

To explain the saturability of the  $\text{CaF}_2:\text{H}^-:\text{Er}^{3+}$  system, we propose a model in which the  $\text{CO}_2$  energy is transferred rapidly from the  $\text{H}^-$  vibration to the  $\text{Er}^{3+}$  crystal field levels by the electron phonon interaction. The occurrence of a bottleneck in the relaxation rate from the  $4.4 \text{ cm}^{-1}$  level to the ground state would account for the anomalous saturation properties of erbium with respect to the other rare earth ions.

The  $\text{CaF}_2:\text{H}^-:\text{Ln}^{3+}$  system, where  $\text{Ln}^{3+}$  is one of the rare earth ions, produces a complex infrared spectrum due to the localized modes of vibration of the hydride ion in sites of different symmetry. In particular the tetragonal ( $C_{4v}$ ) site, in which the charge compensating hydride ion is in the interstitial position nearest the rare earth ion, produces a two line spectrum. The saturation measurements described earlier have shown that the rare earth  $\text{Er}^{3+}$  behaves differently from all the other rare earth ions in that the local mode transition saturates at a relatively low intensity. To explain these results we have proposed that the excited  $\text{H}^-$  ion relaxes rapidly with the excitation energy transferring to the nearby  $\text{Er}^{3+}$  crystal field levels. We propose further that a phonon bottleneck delays the transfer of the energy from the crystal field levels to the phonon bath.

E. ARO Sponsored Publications

1. "Anomalous Absorption in Fluctuating Valence CePd<sub>3</sub>," Bulletin of The American Physical Society 25, 344 (1980), with F.E. Pinkerton, J.W. Wilkins, M.B. Maple and B.C. Sales.
2. "Anomalous Lattice Constant Dependence of Off-Center Displacement of Li<sup>+</sup> in KCl," Bulletin of The American Physical Society 25, 185 (1980), with R.P. Devaty.
3. "Anomalous Absorption in Fluctuating Valence Compounds," Proc. Fourth International Conference on Infrared and Millimeter Waves and Their Applications, S. Perkowitz, ed. (IEEE Cat. No. 79, 1980), p. 244, with F.E. Pinkerton, J.W. Wilkins, M.B. Maple and B.C. Sales.
4. "Anomalous Far Infrared Absorption in Small Metal Particles--Quantum Size Effects," Topical Meeting on the Optical Phenomena Peculiar to Matter of Small Dimensions, University of Arizona, Tucson, Arizona, March 18 - 20, 1980, (Optical Society of American, 1980), p. TuAl-1, with R.P. Devaty.
5. "Corrections to Gor'kov-Eliashberg Equations for Far-Infrared Absorption in Small Metal Particles," Topical Metting on the Optical Phenomena Peculiar to Matter of Small Dimensions, University of Arizona, Tucson, Arizona, March 18 - 20, 1980, (Optical Society of America, 1980), PD1-1.
6. "Comment on Gor'kov and Eliashberg's Theory for Far-Infrared Adsorption by Small Metallic Particles," Physical Review B22, 2123 (1980), with R.P. Devaty.
7. "Comment on the Pressure-Induced Off- to On-Center Transition of Li<sup>+</sup> in KCl," Physical Review B22, 4074 (1980), with R.P. Devaty.
8. "Optical Absorption by Small Metallic Particles," Bulletin of The American Physical Society 26, 209 (1981), with R.P. Devaty.
9. "Nonlinear Properties of Matrix Isolated Tetrahedral Molecules at 10.8  $\mu\text{m}$ ," Topical Meeting on Tuneable Lasers, Keystone, Colorado, April 1 - 3, 1981, with W.E. Moerner and A.R. Chraplyvy.
10. "High-Resolution Spectroscopy of Matrix-Isolated ReO<sub>4</sub><sup>-</sup> Molecules," Optics Letters 6, 254 (1981), with A.R. Chraplyvy and W.E. Moerner.
11. "An Optical Signature at meV Energies for Valence Fluctuation Compounds," Valence Fluctuations in Solids, L.M. Falicov, W. Hanke and M.B. Maple, editors, (North-Holland Publishing Co., 1981), 177, with F.E. Pinkerton, J.W. Wilkins, M.B. Maple and B.C. Sales.
12. "Single-Particle--Collective-Mode Coupling and the Mie Resonance in Small Metallic Particles: Optical Properties of Colloidal Na in NaCl," Physical Review B24, Number 2, 1079 (1981), with R.P. Devaty.

13. "Infrared Hole-Burning Spectroscopy of Matrix-Isolated  $\text{ReO}_4^-$  Molecules," *Optics Letters* 6, 431 (1981), with A.R. Chraplyvy and W.E. Moerner.
14. "Optical Structure Near 20 meV in Valence-Fluctuation Compounds," *Physical Review Letters* 47, 1018 (1981), with F.E. Pinkerton, J.W. Wilkins, M.B. Maple and B.C. Sales.
15. "Anharmonic Relaxation Times of Molecular Vibrational Modes in Alkali Halide Crystals," *Physical Review Letters* 47, 1082 (1981), with W.E. Moerner and A.R. Chraplyvy.
16. "Quantitative FIR Absorptivity Measurements of Metals with Dual Non-Resonant Cavities," submitted to *Infrared Physics*, with F.E. Pinkerton.
17. "Persistent Nonphotochemical Hole-Burning of a Molecular Vibrational Mode in Alkali Halide Lattices," CLEO '82, Advance Program, FK 2, 50 (1982), with W.E. Moerner, R.H. Silsbee, A.R. Chraplyvy and D.K. Lambert.
18. "Effects of Alloying on the Far Infrared Optical Absorption of  $\text{CePd}_3$ ," *Bulletin American Physical society* 27, 276 (1982), with B.C. Webb, F.E. Pinkerton and Mihalisim.
19. "Vibrational Relaxation Dynamics of an IR-Laser-Excited Molecular Impurity Mode in Alkali Halide Lattices," *Bulletin of The American Physical Society* 27, 401 (1982), with W.E. Moerner and A.R. Chraplyvy.
20. " $\text{CO}_2$  Laser Saturation of Local Modes in  $\text{CaF}_2:\text{Er}^{3+}:\text{H}^-$ ," *Bulletin of The American Physical Society* 27, 402 (1982), with J.A. Campbell and G.D. Jones.
21. "Far Infrared Properties of Paraelectric Centers in Li doped KBr," *Bulletin of The American Physical Society* 27, 193 (1982), with L.H. Greene.
22. "Persistent Nonphotochemical Hole-Burning of a Molecular Vibrational Mode in Alkali Halide Lattices," A.R. Chraplyvy, W.E. Moerner, A.J. Sievers and R.H. Silsbee, *Applied Physics* B28, 264 (1982).
23. "Shallow Traps and the D<sup>-</sup> Center in Ge:Sb Far Infrared Photocconductivity Studies Below 1° K," with E.A. Schiff, *Phil. Mag.* B45, 69 (1982).
24. "Persistent Holes in the Spectra of Localized Vibrational Modes in Crystalline Solids," W.E. Moerner, A.J. Sievers, R.H. Silsbee, A.R. Chraplyvy and D.K. Lambert, *Phys. Rev. Lett.* 49, 398 (1982).
25. "Quantitative FIR Absorptivity Measurements of Metals with Dual Non-Resonant Cavities," F.E. Pinkerton and A.J. Sievers, *Infrared Physics* 22, 377 (1982).

26. "Persistent Hole-Burning Observed in a Crystal," W.E. Moerner, A.J. Sievers, R.H. Silsbee, A.R. Chraplyvy and D.K. Lambert, Laser Focus (November) 22 (1982).
27. "Spectral Holes," W.E. Moerner, A.J. Sievers, R.H. Silsbee, A.R. Chraplyvy, and D.K. Lambert, Physics News, 1982, pages 69-70.
28. "Paraelectric Pairs in Lithium Doped KBr," L.H. Greene and A.J. Sievers, Solid State Commun. 44, 1235 (1982).

F. Participating Scientific Personnel

J. Campbell	Visiting Scholar
R.P. Devaty	student
T. Gosnell	student
L.H. Greene	student
L. Hanssen	student
Dr. H. Lengfellner	Visiting Fellow
W.E. Moerner	Ph.D. 1982
F.E. Pinkerton	Ph.D. 1981
E.A. Schiff	Ph.D. 1979
A.J. Sievers	Principal Investigator
Dr. J. Typek	Visiting Fellow
B.C. Webb	student

F. References

1. A.R. Chraplyvy and A.J. Sievers, Optics Letters 3, 112 (1978).
2. R.K. Ahrenkiel, D.J. Dunlavy and A.J. Sievers, IEEE J. Quantum Electron. QE-16, 225 (1980).
3. D.E. Watkins, J.F. Figueira and S.J. Thomas, Optics Letters 5, 169 (1980).
4. R.K. Ahrenkiel, D.J. Dunlavy and A.J. Sievers, Opt. Comm. 32, 403 (1980).
5. F.E. Pinkerton, Far Infrared Optical Studies of Valence Fluctuation Compounds, Ph.D. Thesis, Cornell University, 1981.
6. W.E. Moerner, Vibrational Relaxation Dynamics of an IR-Laser-Excited Molecular Impurity Mode in Alkali Halide Lattices, Ph.D. Thesis, Cornell University, 1982.
7. A.R. Chraplyvy, W.E. Moerner and A.J. Sievers, Optics Letters 6, 254 (1981).
8. A.R. Chraplyvy, W.E. Moerner and A.J. Sievers, Optics Letters 6, 431 (1981).
9. W.E. Moerner, A.R. Chraplyvy and A.J. Sievers, Physical Review Letters 47, 1082 (1981).
10. W.E. Moerner, A.R. Chraplyvy and A.J. Sievers, submitted to Physical Review Letters (1982).
11. D.W. Bereman, Physical Review 130. 2193 (1963).
12. A.S. Barker and A.J. Sievers, Review of Modern Physics 47, Suppl. 2 (1975).
13. F. Bridges and R.S. Russell, Solid State Communications 21 (1977).
14. A. Edgar, G.D. Jones and M.R. Presland, J. Phys. C. 12, 1569 (1979).